A Comparative Repair Study of Thymine- and Uracil-Photodimers with Model Compounds and a Photolyase Repair Enzyme

Jens Butenandt,[a] Robert Epple,[a] Ernst-Udo Wallenborn,[b] André P. M. Eker,[c] Volker Gramlich,[d] and Thomas Carell*[a]

Abstract: Cyclobutane uridine and thymidine dimers with *cis-syn*-structure are DNA lesions, which are efficiently repaired in many species by DNA photolyases. The essential step of the repair reaction is a light driven electron transfer from a reduced FAD cofactor ($FADH^-$) to the dimer lesion, which splits spontaneously into the monomers. Repair studies with UV-light damaged DNA revealed significant rate differences for the various dimer lesions. In particular the effect of the almost eclipsed positioned methyl groups at the thymidine cyclobutane dimer moiety on the splitting rates is unknown. In order to investigate the cleavage vulnerability of thymine and uracil cyclobutane photodimers outside the protein environment, two model compounds, containing a thymine or a uracil dimer and a covalently connected flavin, were prepared and comparatively investigated. Cleavage investigations under internal competition conditions revealed, in contrast to all previous findings, faster repair of the sterically less encumbered uracil dimer. Stereoelectronic effects are offered as a possible explanation. Ab initio calculations and X-ray crystal structure data reveal a different cyclobutane ring pucker of the uracil dimer, which leads to a better overlap of the π*-C(4)−O(4)-orbital with the σ*-C(5)−C(5′)-orbital. Enzymatic studies with a DNA photolyase (*A. nidulans*) and oligonucleotides, which contain either a uridine or a thymidine dimer analogue, showed comparable repair efficiencies for both dimer lesions. Under internal competition conditions significantly faster repair of uridine dimers is observed.

Keywords: DNA photolyases · DNA repair · DNA structures · oligonucleotides · UV photolesions

Introduction

UV irradiation of cells causes the formation of *cis-syn*-cyclobutane pyrimidine dimers through a [2π+2π] cycloaddition of two pyrimidines, located next to each other in the DNA double strand.[1–3] The main lesions are thymidine and cytidine dimers. Cytidine-containing dimers undergo a rapid deamination with a half-life time of approximately 6 h to yield the corresponding uridine-containing photoproducts.[4] The uridine and thymidine photoproducts are pre-mutagenic DNA lesions, which may cause cell death and the degeneration of cells into tumor cells.[4–6] DNA photolyases are flavin-dependent DNA-repair enzymes, which revert cyclobutane dimers in the genome of many organisms. The basis of the repair reaction is a light driven electron transfer from the $FADH^-$ cofactor to the dimer, which cleaves spontaneously as its radical anion.[7, 8] The depletion of the ozone layer[9] and the current threat of increasing skin cancer risks[10] as a result of rising UV-irradiation levels is fueling the interest in the mechanism of the light induced enzymatic repair reaction. In this context, all parameters that 1) determine the efficient molecular recognition of DNA lesions and 2) affect the cleavage rates of the various photolesions, are of particular interest. Both factors determine the repair rate and consequently the chance of survival of organisms living exposed to sunlight. We[11] and others[12] recently showed that *cis-syn*-configured photolesions are much more vulnerable towards electron transfer induced cleavage compared with *trans-syn*- or *trans-anti*-photodimers. Investigations of Sancar and coworkers revealed faster enzymatic repair of thymidine dimers compared with uridine dimers. It was suggested that the two almost eclipsed positioned methyl groups at the thymidine cyclobutane ring destabilize the dimer leading to an increased cleavage vulnerability.[13, 14] Recent quantum chemical studies

[a] Dr. T. Carell, Dr. J. Butenandt, Dr. R. Epple
Laboratorium für Organische Chemie, ETH-Zürich
Universitätstrasse 16, CH-8092 Zürich (Switzerland)
Fax: (+41) 1-632-1109
E-mail: tcarell@org.chem.ethz.ch

[b] Dr. E.-U. Wallenborn
Laboratorium für Physikalische Chemie, ETH-Zürich
Universitätstrasse 16, CH-8092 Zürich (Switzerland)

[c] Dr. A. P. M. Eker
Erasmus University Rotterdam
Department of Cell Biology and Genetics
P.O. Box 1738, NL-3000 DR Rotterdam (The Netherlands)

[d] Prof. Dr. V. Gramlich
Laboratorium für Kristallographie, ETH-Zürich
Universitätstrasse 16, CH-8092 Zürich (Switzerland)

0947-6539/00/0601-0062 $ 17.50+.50/0

of cyclobutane uracil and thymine dimers support the destabilizing effect of the two methyl groups, but question significant changes of the dimer reactivity.[15, 16] Ultrafast spectroscopic studies by Michel-Beyerle and calculations by Rösch and coworkers led to the conclusion that the different repair rates might be caused by a different binding geometry of uridine and thymidine photodimers within the enzyme active site. Different binding geometries could determine the repair rate by influencing the electron transfer processes between the $FADH^-$ cofactor and the corresponding lesion.[17, 18]

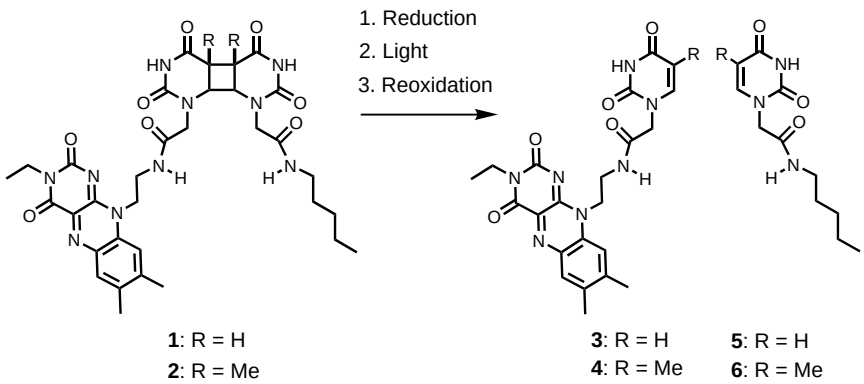

Scheme 1. Light induced cleavage reaction of the two cyclobutane uracil and thymine dimer model compounds **1** and **2** into the reaction products **3**–**6**.

In order to investigate the molecular reasons for the different repair efficiencies in detail, we studied the cleavage rates of uracil and thymine dimers inside and outside the photolyase active site. To this end, the two model compounds **1** and **2** (Scheme 1) were prepared and investigated. In particular, their ability to cleave, in the reduced form, upon exposure to light into **3**–**6** was measured. The obtained cleavage data were compared with competitive and noncompetitive enzymatic repair data obtained with the *A. nidulans* photolyase[19] and uridine and thymidine dimer-containing oligonucleotides.[20, 21] This allowed the determination of the repair rate for both photolesions and enabled to gain initial insight into the molecular recognition of both DNA lesions.

Abstract in German: *Cyclobutan Uridine- und Thymidindimere mit cis-syn-Struktur sind DNA-Schäden, die in vielen Spezies durch DNA-Photolyasen effizient repariert werden. Der entscheidende Schritt der Reparaturreaktion ist ein lichtgetriebener Elektronentransfer von einem reduzierten FAD-Cofaktor ($FADH^-$) auf das Dimer, welches als Radikalanion spontan monomerisiert. Reparaturstudien mit UV-geschädigter DNA ergaben signifikante Unterschiede in den Reparaturraten der verschiedenen Cyclobutan-Dimeren. Unbekannt ist vor allem der Effekt, der zwei beinahe ekliptisch angeordneten Methylgruppen des Thymidin Dimers auf die Reparaturrate. Um die Spaltungseffizienz von Cyclobutan Uracil- und Thymindimeren zu untersuchen, wurden zwei Modellverbindungen dargestellt. Eine vergleichende Spaltungs- (Reparatur) Studie unter internen Konkurrenzbedingungen ergab, im Gegensatz zu allen bisherigen Messungen, eine wesentlich schnellere Reparatur des sterisch weniger belasteten Uracildimers. Als Erklärung schlagen wir stereoelektronische Gründe vor. So zeigen ab initio Berechnungen und Röntgenkristallstrukturdaten eine etwas andere Verzerrung des Uracil-Cyclobutanrings. Dies führt zu einer besseren Überlappung des π^*-C(4)−O(4) Orbitals mit dem σ^*-C(5)−C(5′) Orbital. Enzymatische Untersuchungen mit einer DNA-Photolyase (A. nidulans) und mit Oligonukleotiden, die entweder ein Uridin- oder ein Thymidindimeranalogon enthalten, zeigen vergleichbare Reparaturraten für beide Dimere in der aktiven Tasche. Unter internen Konkurrenzbedingungen wird im Gegensatz hierzu, eine signifikant schnellere Reparatur der Uridindimeren beobachtet.*

Results and Discussion

Synthesis of the model compounds 1 and 2: The preparation of the *cis-syn*-uracil model compound **1** was performed as described recently[11] from the *cis-syn*-uracil dimer diacid **7**,[22–24] flavin **8** and pentylamine **9** (see Scheme 4). For the synthesis of the *cis-syn*-thymine model compound **2**, *N*(1)-carboxymethyl-thymine (**10**) was esterified with benzyl alcohol, as depicted in Scheme 2, to give the thymine benzyl ester **11**. The ester **11** was irradiated in acetone in a standard Pyrex-photochemical apparatus with a medium pressure mercury lamp ($\lambda > 300$ nm) as the light source. During the irradiation a mixture of all four possible isomers **12**–**15** was formed. These were separated by using a combination of selective precipitation, chromatography, and recrystallization as described in the experimental part. Starting material **11** (12 g) yielded the desired *cis-syn*-compound **12** (on average 300 mg) and the *trans-syn*-dimer **13** (approx. 4.5 g).

The X-ray crystal structure analysis (Figure 1) of all four thymine photodimers **12**–**15** allowed the correct structural assignment. Subsequent hydrogenolytic cleavage of the benzyl esters in both compounds **12** and **13** gave the *cis-syn*- and *trans-syn*-thymine dimer dicarboxylic acids **16** and **17**, required for this study, in excellent yields.

The flavin ethylamine building block **8** was prepared as depicted in Scheme 3. *ipso*-Substitution with dinitrodimethylbenzene **18**[25] and mono-Boc-protected ethylene diamine **19** furnished the nitroaniline **20** after chromatography and recrystallization from ethanol in 67%.[26, 27] Compound **19** was prepared in one step from ethylene diamine and Boc_2O.[28] Hydrogenolytic reduction of **20** to **21** and condensation of **21** with alloxan and boric acid in acetic acid, following a general flavin synthesis protocol of Kuhn and co-workers,[29, 30] furnished the flavin compound **22** (80%). Alkylation at *N*(3) in **22** with ethyl iodide and Cs_2CO_3 in dimethylformamide (DMF) gave the flavin derivative **23** after chromatog-

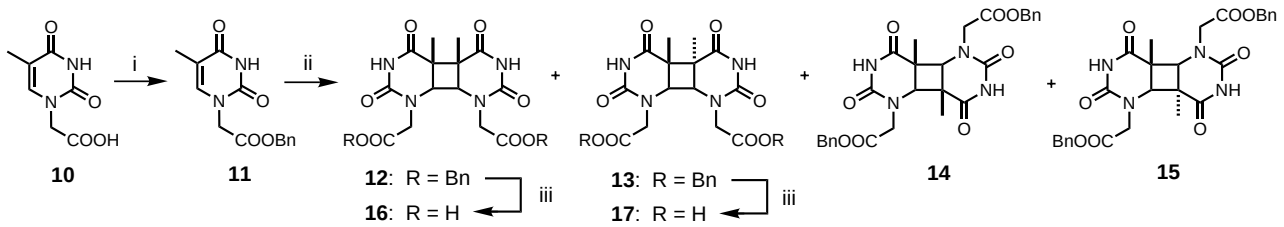

Scheme 2. Synthesis of the cyclobutane thymine dimer building blocks **16** and **17** starting from **10** required for the preparation of the model compounds **2** and **24**. i) BnOH, carbonyldiimidazole (CDI), DMF, RT; ii) $h\bar{\nu} > 300$ nm, acetone, RT; iii) 10% Pd/C catalyst, H_2, HOAc, RT.

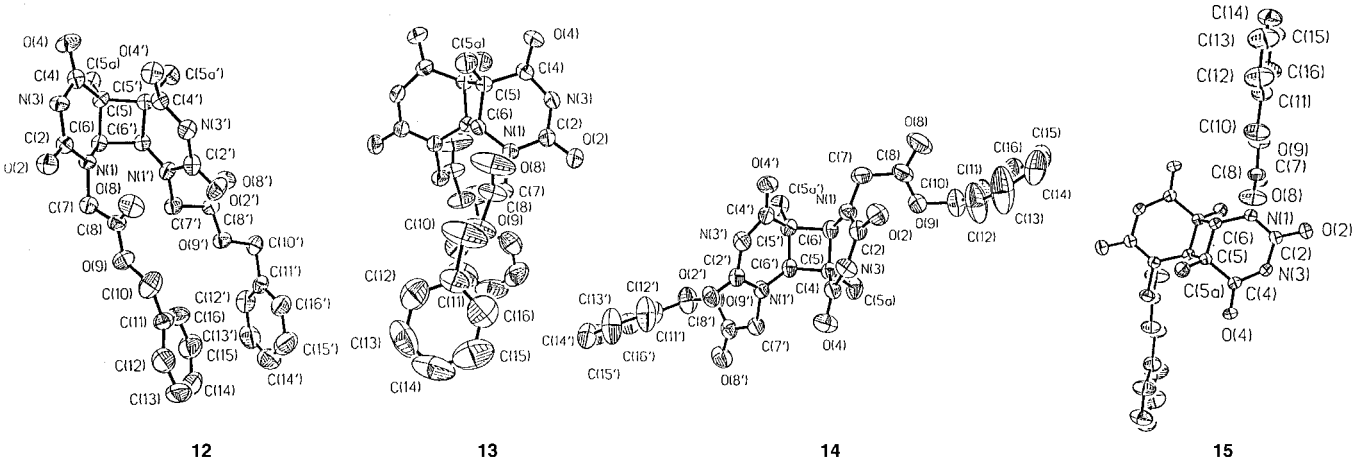

Figure 1. X-ray crystal structures of all four thymine photodimers **12**–**15**. ORTEP plots of the molecular structures. Arbitrary numbering. Displacement ellipsoids are shown at the 50% probability level.

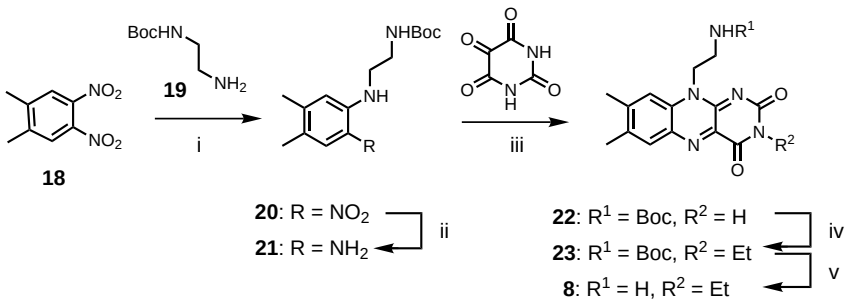

Scheme 3. Synthesis of the aminoethyl substituted flavin building block **8**. i) pyridine, 90 °C, 24 h; ii) 10% Pd/C catalyst, H_2, HOAc, RT; iii) HOAc, $B(OH)_3$, RT; iv) EtI, Cs_2CO_3, DMF, RT; v) TFA, H_2O.

raphy in 71% yield. Cleavage of the *tert*-butyloxycarbonyl (Boc)-protecting group furnished the flavin ethylamine **8** (97%) in an overall yield of 38%.

The preparation of the model compounds **1**, **2**, and **24** (Scheme 4) required activation of the carboxylic acids of **7**, **16**, and **17** with benzotriazol-1-yl-oxy-tris-(dimethylamino)-phosphonium hexafluorophosphate (BOP)[31] in DMF. After addition of one equivalent of the flavin ethylamine **8** and diisopropylethylamine (DIEA), a large excess of pentylamine **9** was added to each reaction mixture. The model compounds **1**, **2**, and **24** (prepared for comparison reasons) were obtained after chromatography on silica gel-H in approximately 30% yield as yellow powders.

Cleavage studies with the uracil dimer- and thymine dimer-containing model compounds 1 and 2: Analysis of the cleavage rates (Scheme 1) of the uracil and the thymine photodimer-containing model compounds **1** and **2** was performed under strictly identical conditions. To this end **1** and **2** were dissolved in various solvents (10^{-5} M or 10^{-6} M). A one to one mixture was prepared and filled into a quartz cuvette stoppered with a rubber septum and equipped with a magnetic stirrer. A small amount of triethylamine (25 μL) was added to ensure deprotonation of the reduced flavin cofactor. The solution was purged with nitrogen for 20 min in order to establish anaerobic conditions. To reduce the flavin chromophore, 20 μL of an aqueous sodium dithionite solution (0.05 M) was added. The assay solution was stirred and irradiated with monochromatic light ($\lambda = 366$ nm). During the irradiation experiment, five to ten 50 μL samples were removed from the assay solution with a micro syringe after defined time intervals. The samples were filled into small vials and subsequently vigorously shaken to reoxidize the flavin cofactor. This helps to stop the cleavage reaction, while the sample is analyzed. All samples were analyzed by reversed-phase HPLC in order to quantify the amount of the model compounds **1** and **2** and of the expected photosplit products **3** and **4**.[11] A representative set of HPLC chromatograms showing the simultaneous cleavage of both model compounds **1** and **2** into **3** and **4** is depicted in Figure 2.

0947-6539/00/0601-0064 $ 17.50+.50/0 *Chem. Eur. J.* **2000**, *6*, No. 1

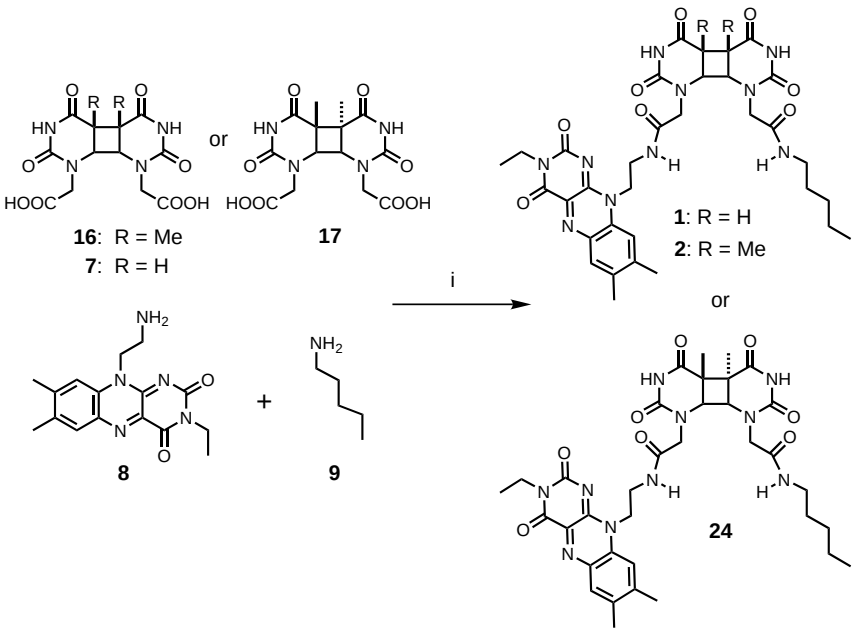

Scheme 4. Synthesis of the flavin-containing photolyase model compounds **1**, **2** and **24**. i) BOP, TEA, DMF, RT.

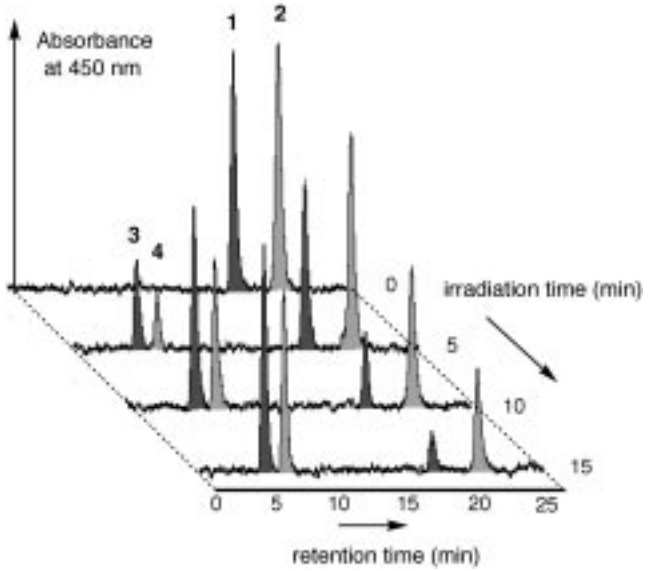

Figure 2. Series of reversed-phase HPLC chromatograms obtained during the light induced conversion of the model compounds **1** and **2** into the cleaved products **3** and **4** (ethylene glycol). The chromatograms show **1** and **2** eluting at approximately 18 min and 21 min, respectively. The cleavage products **3** and **4** elute at approximately 6 min and 8 min, respectively. Conditions: Lichrosphere column (250 × 4) 100/5. Gradient: water/methanol from 70:30 to 10:90 over 30 min. Detection at 450 nm.

Evidently, the two model compounds **1** and **2**, with retention times of 18 min (**1**) and 21 min (**2**), react cleanly to the photosplit products **3** and **4** with retention times of 6 min and 8 min, respectively. The quantitative cleavage rate of both model compounds was obtained from plots of the yields of **3** and **4** against the irradiation time. One representative diagram is shown in Figure 3. The plot shows, in contrast to the current belief, a significantly faster cleavage of the sterically less strained uracil dimer model compound **1**. The cyclobutane uracil dimer was found to cleave by a factor of 2–3 times more rapidly compared with the corresponding thymine dimer. In order to determine the quantum yields for the reactions, the number of photons emitted by the light source into the sample was determined by ferrioxalate actinometry.[32, 33] Together with the absorption of the samples, which were determined by UV/Vis-spectroscopy ($\varepsilon_{\text{flavin,red,366nm}} = 4900\,\text{L mol}^{-1}\,\text{cm}^{-1}$), this value allowed the calculation of the quantum yield Φ (Φ = number of reacted molecules per number of absorbed photons). For the uracil dimer a quantum yield of approximately 4.5% was determined in ethylene glycol as the solvent. The thymine dimer cleaved significantly slower with a quantum yield of about 2.1% (Figure 4).

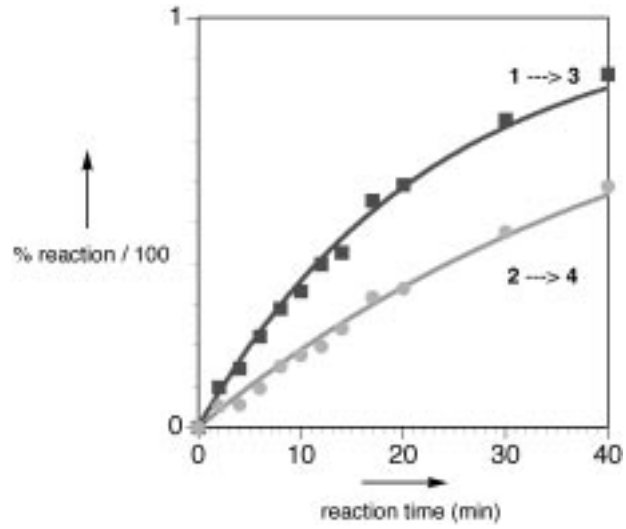

Figure 3. Time-dependent formation of the cleaved photoproducts **3** and **4** during the irradiation of a mixture containing **1** and **2**. Irradiation was performed at 366 nm in ethylene glycol at 25 °C. ■: **3**, ○: **4**.

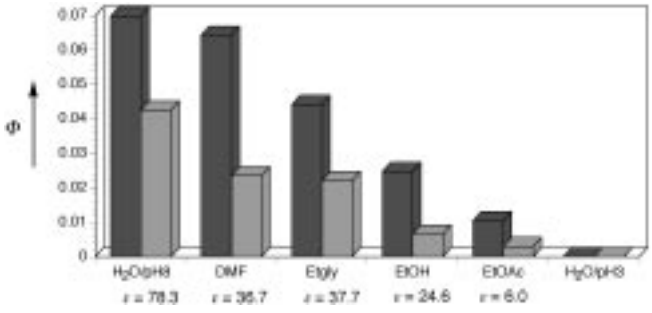

Figure 4. Bar diagrams showing the quantum yields (Φ) for the cleavage process of **1** and **2** reacting to **3** and **4** in various solvents. DMF = dimethylformamide, Etgly = ethylene glycol, EtOH = ethanol, EtOAc = ethyl acetate. Irradiation was performed at $\lambda = 366$ nm at 25 °C. Dark grey bars: uracil model compound **1**. Light grey bars: thymine model compound **2**.

In order to exclude that the surprising cleavage rate difference is influenced by the chosen medium, all measurements were repeated in a variety of solvents including water, ethanol, and ethyl acetate (plus 25 μL triethylamine each).[34] Since the sodium dithionite solution is not miscible with most of these solvents, we reduced the flavin unit by catalytic hydrogenation. To achieve complete reduction, a small amount of $Pd/BaSO_4$ was added into the cuvette as the hydrogenation catalyst. The cuvettes were again purged with nitrogen. Then a stream of hydrogen was passed through the solution. Complete reduction and deprotonation of the flavin cofactor was monitored by UV spectroscopy.[11] The assay solutions were subsequently irradiated at 366 nm and analyzed as described above. The obtained cleavage quantum yields are compiled in Figure 4. We observe moderately reduced cleavage efficiencies in nonpolar solvents, in agreement with earlier data.[11] The fastest cleavage is detected in pure water at pH > 7. No cleavage takes place at pH 3 in agreement with the absolute necessity to deprotonate the reduced flavin chromophore (p*K*a 6.3).[11, 35] Most important, however, is the observation that the uracil dimer-containing model compound **1** cleaves in all investigated solvents by a factor of approximately 2 more efficient. The data obtained in these experiments clearly disprove the current opinion that the two "eclipsed" positioned methyl groups at the thymine dimer cyclobutane ring enforce faster cleavage. In contrast, the sterically less encumbered uracil dimer possesses the higher reductive cleavage vulnerability.

For comparison we also investigated the cleavage rate of the *trans-syn*-thymine dimer model compound **24**. The result of this study is depicted in Figure 5. Clearly evident is the reduced cleavage rate of the *trans-syn*-dimer (factor of 2) compared with the *cis-syn*-configured thymine dimer in model compound **2**. This result is in excellent agreement with data from earlier studies, which showed that *trans-syn*-configured dimers are more stable towards reductive ring opening.[11] This result underlines that the cleavage rate is strongly influenced by the substitution pattern and the configuration of the dimer unit.

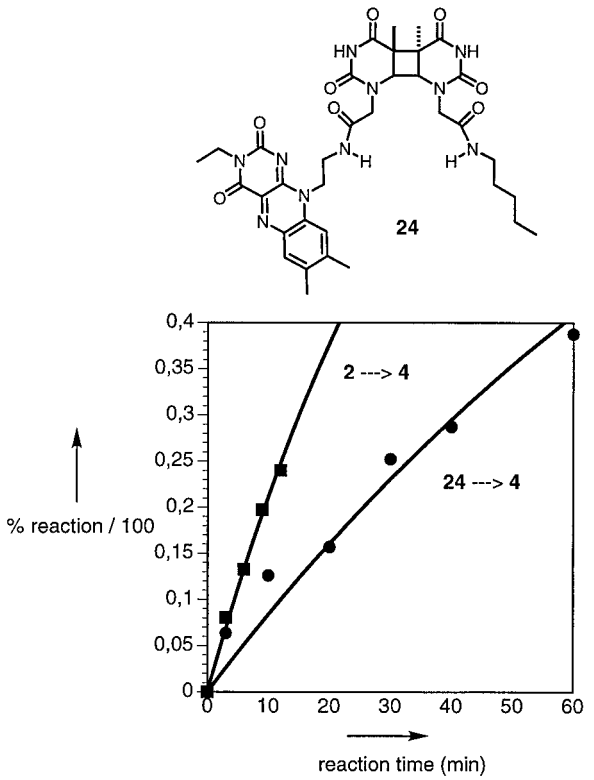

Figure 5. Time-dependent formation of the cleaved photoproduct **4** during the irradiation of **2** and **24**. Irradiation was performed at $\lambda = 366$ nm in ethylene glycol at 25 °C. ■: **4** formed upon irradiation of **2**. ●: **4** formed upon irradiation of **24**.

Enzymatic studies: In order to determine the enzymatic cleavage rates of uridine and thymidine DNA photolesions, we prepared a series of lesion-containing oligonucleotides and investigated their repair efficiencies (Scheme 5). The oligonucleotides **25**–**28**, containing uridine or thymidine photolesion analogues in different base sequence contexts, which are expected to be repaired resulting in **29**–**32**, were prepared by using DNA-lesion phosphoramidite building blocks and solid-phase oligonucleotide synthesis. As the lesion analogues we used the recently described formacetal-linked uridine and thymidine dimers, which are readily available in larger quantities. Both are excellent photolyase substrates.[20, 21] The molecular structures of the building blocks **33** and **34** and the single crystal structure of the thymidine dimer analogue **34** is depicted in Figure 6. In order to investigate the enzymatic repair reaction, the synthesized oligonucleotides were dissolved in 500 μL of a photoreactivation buffer (see Experimental Section). The solutions were filled into a quartz cuvette equipped with a magnetic stirrer. After addition of 50 μL of an enzyme stock solution, the cuvette contained 5×10^{-6} M, 10^{-6} M, or 10^{-7} M DNA, and 2.5×10^{-8} M or 5×10^{-8} M enzyme. The corresponding solution was stirred and irradiated with monochromatic light at 435 nm. 20 μL samples were removed from the assay solution after defined time intervals. Each sample was diluted with 10 μL of 0.1 M acetic acid, to ensure that the cleavage reaction remains stopped during sample analysis. The samples were subsequently vigorously stirred and subjected to reversed-phase or ion-exchange HPLC analysis (nucleosil column 120/3 or nucleogel SAX). This allowed us to quantify the amount of damage-containing oligonucleotide and of enzymatically repaired product.

25: 5'-d(CGACG**T=T**GCAGC)-3' $\xrightarrow{i}$ **29**: 5'-d(CGACG**TT**GCAGC)-3'

26: 5'-d(CGACG**U=U**GCAGC)-3' $\xrightarrow{i}$ **30**: 5'-d(CGACG**UU**GCAGC)-3'

27: 5'-d(CGTAT**T=T**ATTCTGC)-3' $\xrightarrow{i}$ **31**: 5'-d(CGTAT**TT**ATTCTGC)-3'

28: 5'-d(CGTAT**U=U**ATTCTGC)-3' $\xrightarrow{i}$ **32**: 5'-d(CGTAT**UU**ATTCTGC)-3'

Scheme 5. Depiction of the prepared oligonucleotides **25**–**32**. **25**–**28** contain either a uridine dimer analogue (**26** and **28**) or a thymidine analogue (**25** and **27**). Depiction of the repair reaction giving the repaired oligonucleotides **29**–**32**. i) *A. nidulans* photolyase, $h\tilde{\nu} = 435$ nm.

0947-6539/00/0601-0066 $ 17.50+.50/0 *Chem. Eur. J.* **2000**, *6*, No. 1

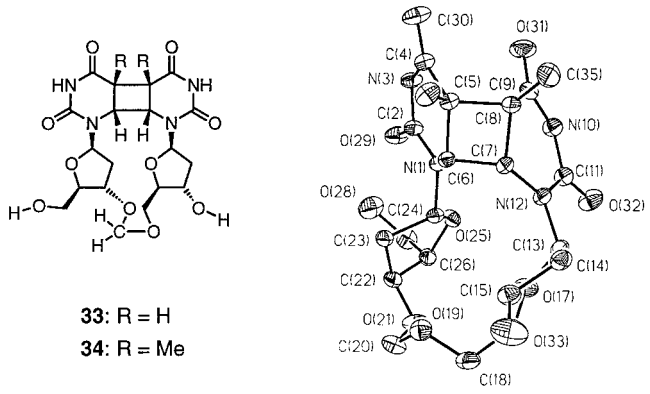

Figure 6. Depiction of the molecular structures of the uridine and thymidine photolesion analogues **33** and **34** used for the enzymatic studies. X-ray crystal structure of the thymidine dimer **34**. For the crystal structure of **33** see ref. [21]. ORTEP plot of the molecular structure. Arbitrary numbering. Displacement ellipsoids are shown at the 50% probability level.

The product peak was integrated and the value plotted against the photoreactivation time. The time point at which 50% of the damaged oligonucleotide was repaired was determined ($t_{1/2}$). These $t_{1/2}$ values are listed in Table 1. The

Table 1. Repair investigation with the oligonucleotides **25**–**28** and the *A. nidulans* photolyase. Irradiation at 435 nm. Buffer: 100 mM NaCl, 10 mM KH_2PO_4, 5 mM DTT, pH 7.0. $t_{1/2}$ is the time at which 50% of the damaged oligonucleotide is repaired.

Substrate	c_{DNA} [M]	c_{enzyme} [M]	$t_{1/2}$ [min]
25[c]	10^{-7}	5×10^{-8}	2.2 ± 0.3[a]
25[c]	10^{-6}	5×10^{-8}	11 ± 1[a]
25[d]	5×10^{-6}	2.5×10^{-8}	23 ± 1[b]
26[c]	10^{-7}	5×10^{-8}	2.1 ± 0.2[a]
26[c]	10^{-6}	5×10^{-8}	12 ± 1[a]
26[d]	5×10^{-6}	2.5×10^{-8}	21 ± 1[b]
27[c]	10^{-7}	5×10^{-8}	1.8 ± 0.2[a]
27[c]	10^{-6}	5×10^{-8}	12 ± 1[a]
27[d]	5×10^{-6}	2.5×10^{-8}	14 ± 1[b]
28[c]	10^{-7}	5×10^{-8}	1.7 ± 0.2[a]
28[c]	10^{-6}	5×10^{-8}	10 ± 1[a]
28[d]	5×10^{-6}	2.5×10^{-8}	13 ± 1[b]

Bandwidth: [a] 1.7 nm, [b] 5.1 nm. [c] Analysis performed using ion-exchange chromatography. [d] Analysis performed using reversed-phase chromatography.

$t_{1/2}$ data show that all four oligonucleotides **25**–**28** are repaired with almost identical efficiency. Throughout all measurements, we determined a similar repair rate for uridine and thymidine dimer-containing oligonucleotides. The observed repair differences are small and close to the error limit of our assay. Since the oligonucleotide concentration was chosen to be far higher (0.1–5 μM) compared with the expected K_m values (K_d in the nM range),[36] we can assume that the enzyme operates under saturation conditions. All experiments were performed additionally at three different substrate concentrations (0.1 μM, 1 μM, and 5 μM). We always obtained comparable results. In summary, the data show that uridine and thymidine photodimers are enzymatically cleaved with similar repair efficiencies.

In order to obtain more data about the enzymatic reaction, the repair of the damaged oligonucleotides **25**–**28** were investigated under direct competition conditions. To this end, uridine and the thymidine dimer-containing oligonucleotides were mixed [(**25**+**28**), (**26**+**27**), (**25**+**26**), (**27**+**28**)] and used as a substrate mixture in the enzymatic assay. The assay was performed as described above. A fine-tuned HPLC gradient enabled the separation of all four oligonucleotides (the two oligonucleotide reactants and products). Under these competitive conditions each oligonucleotide functions as a competitive inhibitor for the other, which allowed us to examine how efficiently both substrates are recognized by the repair enzyme. The repair data ($t_{1/2}$ values) obtained from these measurements are listed in Table 2. In the competition experiments we observed consistently significantly faster repair of the uridine type photolesion. The results show that if the enzyme is confronted with both photolesions at the same time, it repairs the uridine dimer 50–70% more efficiently compared with the thymidine photolesion.

Table 2. Competitive repair investigation of the oligonucleotides **25**–**28** with the *A. nidulans* photolyase. Irradiation at 435 nm. Buffer: 100 mM NaCl, 10 mM KH_2PO_4, 5 mM DTT, pH 7.0. $t_{1/2}$ is the time at which 50% of the damaged oligonucleotide is repaired.

Substrate	c_{DNA} [M]	c_{enzyme} [M]	$t_{1/2}$ (T=T) [min]	$t_{1/2}$ (U=U) [min]
25+**28**[c]	0.5×10^{-6} each	5×10^{-8}	4.0 ± 0.5	2.7 ± 0.5[a]
26+**27**[c]	0.5×10^{-6} each	5×10^{-8}	5.5 ± 0.5	3.8 ± 0.5[a]
27+**28**[d]	2.5×10^{-6} each	2.5×10^{-8}	21 ± 1	13 ± 1[b]
25+**26**[d]	2.5×10^{-6} each	2.5×10^{-8}	24 ± 1	15 ± 1[b]

Bandwidth: [a] 1.7 nm. [b] 5.1 nm. [c] Analysis performed using ion-exchange chromatography. [d] Analysis performed using reversed-phase chromatography.

The noncompetitive enzymatic studies clearly show that the two "eclipsed" methyl groups at the thymidine cyclobutane moiety do not enforce increased cleavage. Both photolesions are repaired with similar rates. The data show that once bound by the enzyme the lesion cleavage rate is identical.

The competitively determined data show that the microbial photolyase[37, 38] used possesses an active site that allows more efficient binding of uridine-type photolesions. The data support the hypothesis that the binding geometry within the active site and not the substitution pattern of the cyclobutane moiety determines the higher enzymatic repair rate of uridine type DNA lesions. This result is in good agreement with recent ultrashort time spectroscopic data of Michel-Beyerle[18] and calculation of Rösch[17], which suggest that the two thymidine methyl groups hinder the thymidine lesion to penetrate as deep as the uridine substrate into the active site.[18]

Calculations: In order to investigate how the structure of the dimer influences the cleavage rate ab initio calculations were performed[11] with the X-ray crystal structural data of **12** and **13** as input geometries for the uracil and thymine dimers in their neutral and radical anion states. The goal of the calculations was to differentiate how structural factors and the binding situation of the dimer lesion in the active site modulate the repair efficiency. To keep the calculations feasible and allow comparison with the uridine and thymidine

lesion analogues, only truncated dimers (without the carboxymethyl substituents) were retained from the X-ray structures (Figure 1). The positions of the hydrogen atoms were subsequently determined by partial optimization, constraining all internal coordinates involving heavy atoms. The currently accepted cleavage scenario includes the donation of an electron first into the π*-orbital of the C(4)=O(4) double bond and subsequent delocalization of electron density into the σ*-C(5)−C(5′)-bond orbital[15, 39], which reduces the activation barrier for the bond cleavage.[40] To approximate the bond order decrease that occurs after the electron uptake, Mayer bond orders[41] of the C(5)−C(5′) bond were calculated in the neutral and radical anion photodimers. The results of these calculation are listed in Table 3. The data show a decrease of the C(5)−C(5′)-bond order after electron donation to all dimers. This bond order decrease is significantly stronger for the *cis-syn*-uracil dimers compared with the *cis-syn*- and the *trans-syn*-thymine dimers. The calculated data are in good agreement with the experimentally observed increased stability of both thymine dimer radical anions in the model compounds. The result shows that the higher reactivity of the uracil dimer is influenced by the structure of the dimer unit, which determines the overlap of the participating orbitals.

Table 3. Calculated UHF/6–31G* Mayer bond orders[41] for the neutral dimers and their radical anions based on truncated X-ray crystal structures of the dibenzyl esters **12** and **13** and for the uridine and thymidine lesion analogues **33** and **34** as input geometries (hydrogen atoms optimized on the RHF/3–21G level). The calculations were performed with the GAMESS(US) package.[48]

Compound	C(5)−C(5′) Neutral dimer	C(5)−C(5′) Anionic dimer
cis-syn-uracil	0.948	0.775
cis-syn-thymine	0.943	0.835
trans-syn-thymine	0.951	0.828
cis-syn-uridine	0.946	0.777
cis-syn-thymidine	0.940	0.807

In order to obtain information about the enzymatic splitting vulnerability of thymidine and uridine dimer, similar calculations (Table 3) were performed for the *cis-syn*-thymidine and the *cis-syn*-uridine photodimers, which were used for the enzymatic repair studies. Here again, all calculations were performed by using truncated and partially optimized X-ray crystal structures (Figure 6). The obtained Mayer bond orders suggest again faster uridine dimer repair. This, however, is not observed. Both dimers were found to be repaired—under noncompetitive conditions—with almost identical efficiency within the accuracy limit of our assay. We explain the discrepancy between the calculated cleavage vulnerabilities and the enzymatic rate data with a possible structural alteration of the dimers if they are placed in the DNA double strand and are bound in the active site. This hypothesis is supported by the observation that the critical cyclobutane dimer ring pucker changes from CB^--observed in all X-ray crystal structures of the dimer monomers-[21, 42] to CB^+ in a DNA duplex environment.[43]

Conclusion

Previous investigations of the repair of thymidine and uridine DNA lesions by DNA photolyases revealed faster repair of the thymidine dimer lesion. Suggested explanations include: 1) a possible additional destabilization of the dimer due to the two almost eclipsed positioned methyl groups at the thymine dimer cyclobutane ring and 2) a different positioning of the thymidine dimer in the photolyase active site, which might effect the electron transfer processes between the dimer lesion and the $FADH^-$ cofactor. In this study, the investigation of the intrinsic cleavage rates of cyclobutane uracil and thymine dimers was performed with the model compounds **1** and **2**. The obtained data clearly show a higher instability of the uracil dimer radical anion. The uracil dimer radical anion was found to cleave by a factor of 2–3 faster under our conditions. This observation is independent of the solvent polarity. The presented measurements show that the two "eclipsed" positioned thymine methyl groups do not increase the lability of the cyclobutane thymine dimer radical anion, which is in good agreement with recent calculations.[15, 16] Based on our own ab initio calculations of the Mayer bond orders[41] of the neutral dimers and their radical anions, we suggest that the cleavage rates are influenced by stereoelectronic parameters. We believe that the better overlap between the π*-orbital of the C(4)=O(4) double bond and the σ*-C(5)−C(5′)-bond orbital in the uracil dimer enhances its reductive cleavage vulnerability. Similar results were calculated for uridine and thymidine photolesions. These dimers were incorporated into oligonucleotides and the repair was investigated with the *A. nidulans* photolyase. Surprisingly we found that both dimer lesion are repaired with almost identical efficiency under substrate saturation conditions. In direct competition experiments, however, significantly faster repair of the uridine-lesion occured, which indicates that cyclobutane uridine photolesions are recognized by the enzyme with higher affinity.

Future studies are now required in order to learn how the DNA sequence and the DNA structure modulates the repair rate. Exact binding constants for the different substrates need to be determined. Data from such experiments could provide further information about the lesion "flipping" process,[20, 28, 44] which seems to be involved in the molecular recognition of photolesions in a DNA-double strand.[45, 46]

Experimental Section

General methods: All materials were obtained from commercial suppliers and were used without further purification. Solvents of technical quality were distilled prior to use. The aqueous buffers were prepared by using deionized distilled water. For reactions under an inert gas atmosphere, nitrogen of standard quality was used. For analytical thin-layer chromatography, precoated glass silica gel plates (Merck $60F_{254}$) were used. The amino compounds were stained with a ninhydrin solution. Flash chromatography was performed on silica gel (Merck 0.040–0.063 mm) and silica gel-H (Fluka, 0.005–0.040 mm). Melting points are uncorrected and were determined on a Büchi Smp 20. IR spectra were recorded on a Perkin–Elmer 1600 and FT-IR with KBr pellets or $CHCl_3$ solutions. UV spectra were recorded on a Varian Cary 5 UV/Vis spectrophotometer in 1 cm quartz cuvettes. Fluorescence spectra and irradiation experiments were

0947-6539/00/0601-0068 $ 17.50+.50/0 *Chem. Eur. J.* **2000**, *6*, No. 1

performed with a Spex 1680 0.22 m double Spectrometer in 1 cm quartz cuvettes. NMR spectra were recorded on a Varian Gemini 200 (200 MHz (^{1}H), 50 MHz (^{13}C)), Varian Gemini 300 (300 MHz (^{1}H), 75 MHz (^{13}C)) and a Bruker AM 500 (500 MHz (^{1}H), 125 MHz (^{13}C)). The chemical shift (δ) is reported in ppm downfield from tetramethylsilane (TMS, $\delta = 0$). Alternatively, the resonance of residual solvent protons were used as the reference. EI-mass spectra, FAB-mass spectra, MALDI-TOF-mass spectra and ESI-mass spectra were measured by the staff of the mass spectrometry facilities of the ETH Zürich on a Hitachi–Perkin–Elmer VG TRIBRID with 70 eV ionization energy (EI), on a ZAB-2 SEQ with 3-nitrobenzyl alcohol as the matrix (FAB), on a Bruker Reflex spectrometer and on a Finnigan TSQ 7000. Elemental analysis were performed by the microanalysis laboratory of the ETH Zürich. HPLC chromatograms were obtained with a Knauer HPLC instrument (HPLC pumps 64, Knauer variable wavelength UV detector, Knauer degasser) with HPLC grade solvents.

X-ray crystal-structure data of **12**: Colorless needles; $C_{28}H_{28}N_4O_8$, $M_r = 548.5$; monoclinic, space group $P2(1)/n$: $D_c = 1.403$ g cm^{-3}, $Z = 4$, $a = 15.003$ (9), $b = 6.258(5)$, $c = 28.09(4)$ Å, $\alpha = 90.00$, $\beta = 99.08$ (9), $\gamma = 90.00$, $V = 2596$ (5) Å^3, CuK$_\alpha$ ($\lambda = 1.54178$ Å) radiation, 2203 reflections collected, $T = 293$ K. The crystal structure was solved by direct methods (SHELXTL PLUS) and refined by full-matrix least-squares analysis by using experimental weights (heavy atoms anisotropic; H-atoms riding model, fixed isotropic). Final ($R(F) = 0.0411$, $wR(F^2) = 0.1063$) for 362 variable and 2099 observed reflections ($F > 3.0$ s(F)).

X-ray crystal-structure data of **13**: Colorless needles; $C_{28}H_{28}N_4O_8$, $M_r = 548.5$; monoclinic, space group $C2/c$: $D_c = 1.373$ g cm^{-3}, $Z = 4$, $a = 18.174$ (13), $b = 8.282$ (3), $c = 18.732$ (11) Å, $\alpha = 90.00$, $\beta = 109.78$ (5), $\gamma = 90.00$, $V = 2653$ (3) Å^3, MoK$_\alpha$ ($\lambda = 0.71073$ Å) radiation, 2413 reflections collected, $T = 293$ K. The crystal structure was solved by direct methods (SHELXTL PLUS) and refined by full-matrix least-squares analysis by using experimental weights (heavy atoms anisotropic; H-atoms riding model, fixed isotropic). Final ($R(F) = 0.0492$, $wR(F^2) = 0.1319$) for 194 variable and 2337 observed reflections ($F > 3.0\sigma(F)$).

X-Ray crystal-structure data of **14**: Colorless needles; $C_{28}H_{28}N_4O_8$, $M_r = 548.5$; monoclinic, space group $P2(1)/c$: $D_c = 1.383$ g cm^{-3}, $Z = 4$, $a = 13.032$ (13), $b = 16.156$ (11), $c = 12.639(8)$ Å, $\alpha = 90.00$, $\beta = 98.02$ (9), $\gamma = 90.00$, $V = 2635$ (4) Å^3, MoK$_\alpha$ ($\lambda = 0.71073$ Å) radiation, 3652 collected reflections, $T = 293$ K. The crystal structure was solved by direct methods (SHELXTL PLUS) and refined by full-matrix least-squares analysis by using experimental weights (heavy atoms anisotropic; H-atoms riding model, fixed isotropic). Final ($R(F) = 0.040$, $wR(F^2) = 0.097$) for 362 variable and 3463 observed reflections ($F > 3.0\sigma(F)$).

X-ray crystal-structure data of **15**: Colorless needles; $C_{28}H_{28}N_4O_8$, $M_r = 548.5$; triclinic, space group $P1$: $D_c = 1.172$ g cm^{-3}, $Z = 1$, $a = 7.611$ (3), $b = 7.980$ (4), $c = 12.368(7)$ Å, $\alpha = 73.56$ (4), $\beta = 87.47$ (4), $\gamma = 67.45$ (3), $V = 663.6$ (6) Å^3, MoK$_\alpha$ ($\lambda = 0.71073$ Å) radiation, 2536 collected reflections, $T = 293$ K. The crystal structure was solved by direct methods (SHELXTL PLUS) and refined by full-matrix least-squares analysis by using experimental weights (heavy atoms anisotropic; H-atoms riding model, fixed isotropic). Final ($R(F) = 0.042$, $wR(F^2) = 0.1202$) for 182 variable and 2345 observed reflections ($F > 3.0$ $\sigma(F)$).

X-ray crystal-structure data of **34**: Colorless needles; $C_{21}H_{30}N_4O_{11}$, $M_r = 514.49$; orthorhombic space group $P2(1)2(1)2(1)$: $D_c = 1.510$ g cm^{-3}, $Z = 4$, $a = 9.787$ (4), $b = 13.127$ (4), $c = 17.620$ (5) Å, $\alpha = 90.00$, $\beta = 90.00$, $\gamma = 90.00$, $V = 2263.7$ (13) Å^3, MoK$_\alpha$ ($\lambda = 0.71073$ Å) radiation, 4576 collected reflections, $T = 293$ K. The crystal structure was solved by direct methods (SHELXTL PLUS) and refined by full-matrix least-squares analysis by using experimental weights (heavy atoms anisotropic; H-atoms riding model, fixed isotropic). Final ($R(F) = 0.0312$, $wR(F^2) = 0.0756$) for 446 variable and 4576 observed reflections ($F > 3.0\sigma(F)$).

Crystallographic data (excluding structure factors) for the structures reported in this paper have been deposited with the Cambridge Crystallographic Data Centre as supplementary publication no. CCDC-119735 (**12**), CCDC-119738 (**13**), CCDC-119734 (**14**), CCDC-119737 (**15**), CCDC-119736 (**34**). Copies of the data can be obtained free of charge on application to CCDC, 12 Union Road, Cambridge CB2 1EZ, UK (Fax: (+44) 1223-336-033; E-mail: deposit@ccdc.cam.ac.uk).

1,2,3,4-Tetrahydro-5-methyl-2,4-dioxopyrimidine-1-acetic acid (10):[47] Thymine (10.00 g, 79.3 mmol) was suspended in H_2O (150 mL). 50 mL of an aqueous KOH-solution (3.6 M) was added. The mixture was stirred at room temperature until a clear solution was obtained. Chloroacetic acid (15.00 g, 159 mmol) was added and the reaction mixture was heated to reflux for 90 min. The cold reaction mixture was acidified with conc. HCl until pH 1 was reached and kept at 4 °C overnight. The crystallized product **10** was filtered off and dried in vacuo over P_2O_5 (12.50 g, 86 %). M.p.: 285–287 °C (Lit.: 287 °C[47]); ^{1}H NMR (200 MHz, [D$_6$]DMSO): $\delta = 4.42$ (s, 3H), 5.20 (s, 2H), 5.62 (d, $J = 7.9$ Hz, 1H), 7.60 (d, $J = 7.9$ Hz, 1H), 11.33 (s, 1H).

Benzyl-1,2,3,4-tetrahydro-5-methyl-2,4-dioxopyrimidine-1-acetate (11): 1,2,3,4-Tetrahydro-5-methyl-2,4-dioxopyrimidine-1-acetic acid (**10**) (10 g, 54.3 mmol) and 1,1′-carbonylbis[1*H*]-diimidazole (12 g, 74.0 mmol) were stirred in DMF (80 mL) at room temperature. After 15 minutes, benzyl alcohol (8 g, 76.1 mmol) was added and the reaction mixture was stirred for 35 h at RT. The reaction mixtures was concentrated in vacuo and the residual material was suspended in H_2O (50 mL) and filtered off. Recrystallization of **11** from MeOH yielded **11** as colorless plates (14.5 g, 97 %). R_f ($CHCl_3$/MeOH 10:1): 0.65; m.p.: 179–181 °C; IR (KBr): 3156*m*, 3043*m*, 2944*m*, 1737*s*, 1693*s*, 1650*s*, 1458*m*, 1420*m*, 1387*m*, 1360*m*, 1224*s*, 1150*m*, 958*m*, 894*w*, 865*w*, 793*w*, 757*s*; ^{1}H NMR (400 MHz, [D$_6$]DMSO): $\delta = 1.76$ (s, 3H), 4.55 (s, 2H), 5.19 (s, 2H), 7.38 (m, 5H), 7.53 (s, 1H), 11.41 (s, 1H); ^{13}C NMR (100 MHz, [D$_6$]DMSO): $\delta = 11.79$, 48.38, 66.34, 108.56, 127.86 (2C), 128.12, 128.38 (2C), 135.46, 141.45, 150.89, 164.21, 168.11; MS (EI): *m/z* (%): 274 (19) [*M*]$^+$, 167 (17), 139 (57), 91 (100), 65 (7), 41 (9), 28 (12); $C_{14}H_{14}N_2O_4$ (274.28): calcd: C 61.31, H 5.14, N 10.21, found: C 61.25, H 5.34, N 10.18.

Irradiation of 11: The benzyl ester **11** (2.00 g, 7.3 mmol) was dissolved in acetone (200 mL) and the solution was degassed for 15 min in an ultrasonic bath and another 15 min outside the ultrasonic bath by purging nitrogen through the solution. The solution was irradiated for 3 h with a 150 W Hg medium pressure lamp in a standard photochemical apparatus (Pyrex). During the irradiation the solution was purged with nitrogen. The reaction mixture was filtered, evaporated to dryness in vacuo and the product was precipitated with acetone and filtrated. The residual solid material contained mainly **13** and **15**. The filtrate was subjected to column chromatography (silica gel 60, d = 3 cm, L = 18 cm, CH_2Cl_2/acetone 7:1 → 5:1) to yield the residual amounts of the isomers **13** and **15** well separated as white powders and a mixture of the isomers **12** and **14**. Separation of the mixture, containing **12** and **14**, was achieved by column chromatography (silica gel 60, d = 3 cm, L = 18 cm $CHCl_3$/methanol 15:1). Recrystallization of the isomers **13** and **15** from HCOOH/H_2O and of **12** and **14** from methanol yielded all four isomers in analytically pure form.

Dibenzyl-*cis*-[4*a*]-*transoid*-[4*a*,4*b*]-*cis*-[4*b*]-dodecahydro-9,11-dimethyl-2,4,6,8-tetraoxocyclobuta[1,2-*d*:3,4-*d*′]dipyrimidine-1,5-diacetate (15): 200 mg (35 %); R_f ($CHCl_3$/MeOH 10:1) = 0.73; m.p.: 242–244 °C; IR (KBr): 3429*m*, 3233*m*, 3067*w*, 1744*m*, 1711*s*, 1683*s*, 1473*m*, 1389*m*, 1356*w*, 1283*m*, 1256*w*, 1224*m*, 982*w*, 756*w*, 735*w*; ^{1}H NMR (400 MHz, [D$_6$]DMSO): $\delta = 1.25$ (s, 6H), 3.61 (d, $J = 17.5$ Hz, 2H), 3.95 (s, 2H), 4.44 (d, $J = 17.5$ Hz, 2H), 5.13 (d, $J = 12.4$ Hz, 2H), 5.18 (d, $J = 12.4$ Hz, 2H), 7.37 (s, 10H), 10.78 (s, 2H); ^{13}C NMR (100 MHz, [D$_6$]DMSO): $\delta = 17.91$, 44.67, 47.13, 61.38, 66.26, 127.91 (2C), 128.09, 128.34, 135.50, 151.46, 168.02, 172.63; MS (pos. FAB): *m/z* (%): 549 (10, [*M* + H]$^+$), 491 (10), 338 (28); $C_{28}H_{28}N_4O_8$ (548.56): calcd C 61.31, H 5.14, N 10.21; found: C 61.28, H 5.32, N 10.16.

Dibenzyl-*cis*-[4*a*]-*transoid*-[4*a*,4*b*]-*cis*-[4*b*]-dodecahydro-11,12-dimethyl-2,4,5,7-tetraoxocyclobuta[1,2-*d*:4,3-*d*′]dipyrimidine-1,8-diacetate (13): 750 mg (38 %); R_f ($CHCl_3$/MeOH 10:1) = 0.58; m.p.: 204–206 °C; IR (KBr): 3430*m*, 3178*w*, 3065*w*, 2856*w*, 1745*s*, 1700*s*, 1687*s*, 1478*s*, 1388*w*, 1378*w*, 1358*m*, 1284*m*, 1208*s*, 956*w*, 754*w*, 698*w*; ^{1}H NMR (400 MHz, [D$_6$]DMSO): $\delta = 1.23$ (s, 6H), 3.98 (s, 2H), 4.09 (d, $J = 17.7$ Hz, 2H), 4.25 (d, $J = 17.7$ Hz, 2H), 5.11 (d, $J = 12.5$ Hz, 2H), 5.15 (d, $J = 12.5$ Hz, 2H), 7.36 (m, 10H), 10.65 (s, 2H); ^{13}C NMR (100 MHz, [D$_6$]DMSO): $\delta = 20.82$, 45.66, 48.17, 63.32, 66.12, 127.90, 128.08, 128.35, 135.51, 151.31, 169.17, 170.73; MS (pos. FAB): *m/z* (%): 549 (100, [*M* + H]$^+$), 338 (55); $C_{28}H_{28}N_4O_8 + 0.5\,H_2O$ (557.56): calcd C 60.32, H 5.24, N 10.05; found: C 60.59, H 5.30, N 10.34.

Dibenzyl-*cis*-[4*a*]-*cisoid*-[4*a*,4*b*]-*cis*-[4*b*]-dodecahydro-9,11-dimethyl-2,4,6,8-tetraoxocyclobuta[1,2-*d*:3,4-*d*′]dipyrimidine-1,5-diacetate (14): 50 mg (2.5 %); R_f ($CHCl_3$/MeOH 10:1) = 0.55; m.p.: 215–217 °C; IR (KBr): 3433*m*, 3078*w*, 2967*w*, 1744*m*, 1710*s*, 1633*w*, 1475*m*, 1456*w*, 1389*w*, 1356*w*, 1300*w*, 1244*m*, 1194*m*, 961*w*, 756*w*, 700*w*; ^{1}H NMR (400 MHz, [D$_6$]DMSO): $\delta = 1.43$ (s, 6H), 3.74 (s, 2H), 3.84 (d, $J = 17.6$ Hz, 2H), 4.48 (d, $J = 17.6$ Hz, 2H), 5.14 (d, $J = 12.4$ Hz, 2H), 5.19 (d, $J = 12.4$ Hz, 2H), 7.38

(m, 10H), 10.57 (s, 2H); ^{13}C NMR (100 MHz, [D$_6$]DMSO): δ = 20.82, 47.56, 47.87, 61.49, 66.13, 127.89 (2C), 128.07, 128.34 (2C), 135.57, 151.01, 168.58, 170.71; MS (pos. FAB): *m/z* (%): 549 (100, $[M+H]^+$), 491 (8), 338 (45); $C_{28}H_{28}N_4O_8$ (548.56): calcd C 61.31, H 5.14, N 10.21; found: C 61.03, H 5.24, N 10.34.

Dibenzyl-*cis*-[4*a*]-*cisoid*-[4*a*,4*b*]-*cis*-[4*b*]-dodecahydro-11,12-dimethyl-2,4,5,7-tetraoxocyclobuta[1,2-*d*:4,3-*d*′]dipyrimidine-1,8-diacetate (12): 40 mg (2%); R_f ($CHCl_3$/MeOH 10:1) = 0.50; m.p.: 146–148 °C; IR (KBr): 3411*w*, 3217*w*, 3078*w*, 2956*w*, 1744*s*, 1709*s*, 1475*m*, 1391*w*, 1361*w*, 1287*m*, 1194*m*, 965*w*, 754*w*, 698*w*; ^{1}H NMR (400 MHz, [D$_6$]DMSO): δ = 1.31 (s, 6H), 3.92 (d, J = 17.4 Hz, 2H), 3.99 (s, 2H), 4.29 (d, J = 17.4 Hz, 2H), 5.12 (d, J = 12.5 Hz, 2H), 5.18 (d, J = 12.5 Hz, 2H), 7.36 (s, 10H), 10.53 (s, 2H); ^{13}C NMR (100 MHz, [D$_6$]DMSO): δ = 18.18, 46.09, 47.15, 59.34, 66.07, 127.82 (2C), 128.05, 128.33 (2C), 135.56, 152.17, 168.54, 170.34; MS (pos. FAB): *m/z* (%): 549 (100, $[M+H]^+$), 338 (18); $C_{28}H_{28}N_4O_8$ (548.56): calcd C 61.31, H 5.14, N 10.21; found: C 61.37, H 5.28, N 10.15.

***cis*-[4*a*]-*transoid*-[4*a*,4*b*]-*cis*-[4*b*]-Dodecahydro-2,4,5,7-tetraoxo-cyclobuta[1,2-*d*:4,3-*d*′]dipyrimidine-1,8-diacetic acid (17)**: The diester **13** (300 mg, 0.547 mmol) was dissolved in acetic acid (20 mL). After the addition of 10% Pd/C catalyst (10 mg) the suspension was stirred in an H_2 atmosphere for 2 h. The reaction mixture was filtered through Celite. The Celite pad was washed with hot acetic acid twice. The combined filtrates were concentrated in vacuo. The product precipitated upon addition of diethyl ether to the residual oily material and was filtered off, washed with acetone and dried in vacuo to yield a colorless powder (185 mg, 92%). M.p.: 243–245 °C; IR (KBr): 3600–2800*m*, 3400*w*, 3231*w*, 3067*w*, 2867*w*, 1761*m*, 1693*s*, 1483*s*, 1385*m*, 1302*m*, 1239*m*, 1160*m*, 883*w*, 822*w*, 759*w*; ^{1}H NMR (400 MHz, [D$_6$]DMSO): δ = 1.27 (s, 6H), 3.89 (s, 2H), 3.97 (d, J = 17.6 Hz, 2H), 4.04 (d, J = 17.6 Hz, 2H), 10.55 (s, 2H), 11–13 (br s, 2H); ^{13}C NMR (100 MHz, [D$_6$]DMSO): δ = 21.02, 45.60, 48.40, 63.69, 151.24, 170.63, 170.76; MS (pos. FAB): *m/z* (%): 369 (20, $[M+H]^+$), 338 (100), 273 (24), 165 (30); $C_{14}H_{16}N_4O_8$+0.5 CH_3COOH (398.33): calcd C 45.23, H 4.55, N 14.07; found: C 44.94, H 4.87, N 14.05.

***cis*-[4*a*]-*cisoid*-[4*a*,4*b*]-*cis*-[4*b*]-dodecahydro-2,4,5,7-tetraoxo-cyclobuta-[1,2-*d*:4,3-*d*′]dipyrimidine-1,8-diacetic acid (16)**: The diester **12** (250 mg, 0.456 mmol) was dissolved in acetic acid (20 mL). After the addition of 10% Pd/C catalyst (10 mg) the solution was stirred in an H_2 atmosphere for 2 h. The reaction mixture was filtered through Celite and the Celite pad was washed with hot acetic acid. The combined acetic acid solutions were concentrated in vacuo. Addition of diethylether to the oily residual material yielded **16** as a colorless powder. The product was filtered off, washed with acetone and dried in vacuo (168 mg, 100%). M.p.: 229–231 °C; IR (KBr): 3600–2800*m*, 3433*w*, 3222*w*, 3067*w*, 1703*s*, 1486*s*, 1396*m*, 1290*m*, 1219*m*, 1194*m*, 800*w*, 772*w*, 756*w*; ^{1}H NMR (400 MHz, [D$_6$]DMSO): δ = 1.34 (s, 6H), 3.65 (d, J = 17.3 Hz, 2H), 3.94 (s, 2H), 4.16 (d, J = 17.3 Hz, 2H), 10.41 (s, 2H), 12.5–13.5 (br s, 2H); ^{13}C NMR (100 MHz, [D$_6$]DMSO): δ = 18.23, 46.19, 47.07, 59.22, 152.12, 170.00, 170.51; MS (pos. FAB): *m/z* (%): 369 (64, $[M+H]^+$), 338 (100).

***N*-*tert*-Butyloxycarbonyl-ethylene diamine (19)**:[28] A solution of Boc_2O (30 g, 0.14 mol) in 1,4-dioxane (100 mL) was added dropwise within 2 h at room temperature to a solution of ethylene diamine (25.0 g, 0.42 mol) in 1,4-dioxane (150 mL). The reaction mixture was stirred for another 20 h at room temperature. The reaction mixture was filtered and the filtrate was concentrated in vacuo. The residual oil was distilled and the product **19** was isolated at 105 °C (20 Torr) and obtained as a colorless oil (13 g, 62%) and used without further purification. ^{1}H NMR (300 MHz, $CDCl_3$): δ = 1.19 (s, 2H), 1.38 (s, 9H), 2.72 (t, J = 6.0 Hz, 2H), 3.10 (m, 2H), 5.20 (br s, 1H).

***N*-[2-({[(*tert*-Butyl)oxy]carbonyl}amino)ethyl]-4,5-dimethyl-2-nitro-aniline (20)**: The mono-Boc protected ethylene diamine (**19**) (6.3 g, 39.3 mmol) was dissolved in pyridine (15 mL). This solution was slowly added to a solution of 1,2-dinitro-4,5-dimethylbenzene (**18**) (5 g, 25.5 mmol) in pyridine (50 mL). The reaction mixture was stirred for 24 h at 90 °C and subsequently concentrated in vacuo. The residual material was recrystallized from ethanol. This yielded **20** as intensively red-colored needles (5.3 g, 67%). R_f (toluene/EtOAc 10:1) = 0.33; m.p.: 120–122 °C; IR (KBr): 3378*m*, 3356*m*, 2978*w*, 2933*w*, 1683*s*, 1639*m*, 1572*m*, 1528*s*, 1511*m*, 1461*w*, 1400*w*, 1367*w*, 1344*w*, 1311*w*, 1294*w*, 1289*w*, 1250*w*, 1222*m*, 1194*s*, 1172*m*, 1150*s*, 1033*w*, 1000*w*, 861*w*; ^{1}H NMR (400 MHz, $CDCl_3$): δ = 1.37 (s, 9H), 2.14 (s, 3H), 2.25 (s, 3H), 3.19 (q, J = 6.0 Hz, 2H), 3.38 (m, J = 5.8 Hz, 2H), 6.93 (s, 1H), 7.01 (t, J = 5.3 Hz, 1H), 7.82 (s, 1H), 8.09 (t, J = 5.8 Hz, 1H); ^{13}C NMR (100 MHz, $CDCl_3$): δ = 17.94, 20.08, 28.08 (3C), 38.82, 42.23, 77.70, 114.48, 124.01, 125.35, 128.86, 143.81, 147.31, 155.86; MS (EI): *m/z* (%): 309 (3, $[M]^+$), 179 (100), 57 (47); $C_{15}H_{23}N_3O_4$ (309.37): calcd C 58.24, H 7.49, N 13.58; found: C 58.35, H 7.52, N 13.52.

10-[2-({[(*tert*-Butyl)oxy]carbonyl}amino)ethyl]-7,8-dimethyl-[3*H*,10*H*]-benzo[g]pteridine-2,4-dione (22): A suspension of 10% Pd/C catalyst (100 mg) in acetic acid (10 mL) was slowly added to a solution of the nitro compound **20** (3.0 g, 9.70 mmol) in methanol (150 mL). The suspension was stirred for 7 h at room temperature in an H_2 atmosphere. The reaction mixture containing **21** was filtered through Celite. To the filtrate was added alloxan monohydrate [2,4,5,6(1*H*,3*H*)-pyrimidinetetrone] (8 g, 50 mmol) and boric acid (14 g, 230 mmol) and the reaction mixture was stirred for 12 h at room temperature. The reaction mixture was diluted with $CHCl_3$ (500 mL) and extracted with water (3 × 250 mL). The organic phase was separated, dried with $MgSO_4$, and concentrated in vacuo. The product **22** was obtained after column chromatography (silica gel-H, d = 3 cm, L = 15 cm, $CHCl_3$/MeOH 15:1 → 10:1 and recrystallization from ethanol/1,4-dioxane as orange-colored needles (3.02 g, 80%). R_f ($CHCl_3$/MeOH 10:1) = 0.46; m.p.: 212–214 °C; IR ($CHCl_3$): 3456*w*, 3378*w*, 3007*w*, 1712*m*, 1683*m*, 1581*m*, 1548*s*, 1506*m*, 1458*w*, 1394*w*, 1368*w*, 1344*w*, 1294*w*, 1272*w*, 1164*m*, 867*w*; ^{1}H NMR (400 MHz, [D$_6$]DMSO): δ = 1.23 (s, 9H), 2.40 (s, 3H), 2.49 (s, 3H), 3.41 (q, J = 6.0 Hz, 2H), 4.64 (t, J = 6.0 Hz, 2H), 6.96 (t, J = 6.0 Hz, 1H), 7.83 (s, 1H), 7.89 (s, 1H), 8.31 (s, 1H); ^{13}C NMR (100 MHz, [D$_6$]DMSO): δ = 18.67, 20.75, 27.94 (3C), 36.82, 44.13, 79.13, 116.17, 130.91, 131.44, 133.85, 135.62, 136.82, 146.26, 150.35, 155.46, 155.76, 159.86; MS (EI): *m/z* (%): 385 (1, $[M]^+$), 312 (10), 256 (9), 243 (100), 84 (28), 49 (31); $C_{19}H_{23}N_5O_4$ (385.42): calcd C 59.21, H 6.01, N 18.17; found: C 59.35, H 6.12, N 18.29.

10-[2-({[(*tert*-Butyl)oxy]carbonyl}amino)ethyl]-7,8-dimethyl-3-ethyl-[3*H*,10*H*]-benzo[g]pteridine-2,4-dione (23): Ethyl iodide (1 mL, 12.37 mmol) were dropwise added to a suspension of the flavin derivative **22** (500 mg, 1.3 mmol) and Cs_2CO_3 (0.6 g, 1.83 mmol) in dry (4 Å mol sieves) DMF (50 mL). The reaction mixture was stirred at room temperature for 3 h. The mixture was diluted with $CHCl_3$ (200 mL) and extracted with water (3 × 80 mL). The organic phase was separated, dried with $MgSO_4$, filtered, and evaporated in vacuo. The product **23** was obtained after flash chromatography on silica gel-H (d = 3 cm, L = 18 cm, $CHCl_3$/MeOH 20:1) and recrystallization from MeOH/H_2O as yellow needles (380 mg, 71%). R_f ($CHCl_3$/MeOH 20:1) = 0.41; m.p.: 227–229 °C; IR ($CHCl_3$): 3398*w*, 2977*w*, 2933*w*, 1706*m*, 1693*m*, 1644*s*, 1583*s*, 1545*m*, 1447*w*, 1433*w*, 1337*m*, 1311*w*, 1294*w*, 1272*w*, 1250*m*, 1200*w*, 1176*m*, 1017*w*, 994*w*, 933*w*, 889*w*, 806*q*, 772*w*; ^{1}H NMR (400 MHz, [D$_6$]DMSO): δ = 1.16 (t, J = 7.0 Hz, 3H), 1.22 (s, 9H), 2.40 (s, 3H), 2.50 (s, 3H), 3.41 (q, J = 5.7 Hz, 2H), 3.93 (t, J = 7.0 Hz, 2H), 4.66 (t, J = 5.7 Hz, 2H), 6.98 (t, J = 5.7 Hz, 1H), 7.86 (s, 1H), 7.93 (*s*, 1H); ^{13}C NMR (100 MHz, [D$_6$]DMSO): δ = 12.83, 18.63, 20.71, 27.86 (3C), 35.82, 36.90, 43.95, 77.75, 116.10, 130.87, 131.33, 134.10, 135.69, 135.86, 146.40, 148.87, 154.40, 155.69, 159.09; MS (FAB): *m/z* (%): 414 (100, $[M+1]^+$), 358 (6), 340 (8), 271 (36); $C_{21}H_{27}N_5O_4 + \frac{2}{3}H_2O$ (425.49): calcd C 59.28, H 6.71, N 16.46; found: C 59.21, H 6.65, N 16.29.

10-(2-Aminoethyl)-7,8-dimethyl-3-ethyl-[3*H*,10*H*]-benzo[g]pteridine-2,4-dione, TFA salt (8): A solution of the Boc-protected flavin derivative **23** (437 mg, 1.03 mmol) in TFA/water (10 mL 95:5) was stirred for 3 h at room temperature. The reaction solution was evaporated in vacuo and the product was precipitated through addition of diethyl ether. Compound **8** was obtained as the TFA salt in form of a yellow powder (427 mg, 97%). IR ($CHCl_3$): 3444*m*, 1713*s*, 1615*s*, 1580*s*, 1542*s*, 1458*m*, 1347*m*, 1250*s*, 1193*m*, 1022*w*, 929*w*, 878*w*, 806*w*, 773*w*; ^{1}H NMR (300 MHz, [D$_6$]DMSO): δ = 1.16 (t, J = 6.9 Hz, 3H), 2.42 (s, 3H), 2.50 (s, 3H), 3.20 (m, 2H), 3.94 (q, J = 6.9 Hz, 2H), 4.91 (t, J = 6.0 Hz, 2H), 7.98 (s, 1H), 8.05 (s, 1H), 8.17 (m, 3H); ^{13}C NMR (75 MHz, [D$_6$]DMSO): δ = 12.82, 18.63, 20.41, 35.93, 35.99, 41.11, 116.05, 130.68, 131.28, 134.30, 136.20, 136.46, 147.31, 149.63, 154.68, 159.25; MS (FAB): *m/z* (%): 314 (100, $[M-CF_3COO]^+$), 271 (15), 232 (7).

Model compound 2: A solution of the *cis-syn*-thymine dimer dicarboxylic acid **16** (55 mg, 0.15 mmol) and an excess of BOP (300 mg, 0.646 mmol) were dissolved in DMF (4 mL) and stirred at room temperature for 10 min. After the addition of a solution of **8·TFA** (50 mg, 0.17 mmol) in DMF (2 mL) and of ten drops of triethylamine, the reaction was stirred for 2 h at room temperature. Then pentyl alcohol **9** (40 mg, 0.38 mmol) was added to the reaction mixture, and stirring was continued for another 4 h at room temperature. The reaction mixture was diluted with water (100 mL) and extracted with $CHCl_3$ (3 × 200 mL). The combined organic layers were

0947-6539/00/0601-0070 $ 17.50+.50/0 *Chem. Eur. J.* **2000**, *6*, No. 1

separated, dried with $MgSO_4$, filtrated, and concentrated in vacuo. The crude reaction product was dissolved in a small amount of methanol and precipitated through addition of diethyl ether. The product was purified by silica gel column chromatography (silica gel-H, d = 3 cm, L = 20 cm, $CHCl_3$/MeOH 7.5:1 →5:1. **2** was obtained as a yellow powder (38 mg, 35 %). R_f ($CHCl_3$/MeOH 10:1): 0.22; m.p. : 240 – 242 °C; IR (KBr): 3430*m*, 3211*m*, 3078*w*, 2933*w*, 2856*w*, 1704*s*, 1650*s*, 1584*m*, 1548*s*, 1465*m*, 1389*w*, 1282*m*, 1228*m*, 1017*w*, 928*w*, 806*w*; ^{1}H NMR (500 MHz, [D$_6$]DMSO): δ = 0.86 (t, J = 7.1 Hz, 3H), 1.15 (t, J = 7.0 Hz, 3H), 1.26 (m, 4H), 1.31 (s, 3H), 1.36 (s, 3H), 1.37 (m, 2H), 2.42 (s, 3H), 2.52 (s, 3H), 3.05 (m, 2H), 3.34 (m, 1H), 3.49 (m, 2H), 3.79 (d, J = 5.2 Hz, 1H), 3.87 (d, J = 5.2 Hz, 1H), 3. 91 (m, 1H), 3.93 (q, J = 7.1 Hz, 2H), 4.15 (d, J = 16.5 Hz, 1H), 4.20 (d, J = 16.5 Hz, 1H), 4.61 (m, 1H), 4.73 (m, 1H), 7.92 (s, 1H), 7.93 (t, J = 5.6 Hz, 1H), 7.97 (s, 1H), 8.22 (t, J = 6.0 Hz, 1H), 10.36 (s, 1H), 10.39 (s, 1H); ^{13}C NMR (125 MHz, [D$_6$]DMSO): δ = 12.82, 13.80, 18.06, 18.21, 18.66, 20.70, 21.72, 28.46, 28.66, 35.76, 35.88, 38.44, 42.91, 46.34, 46.57, 47.77, 47.84, 59.30, 59.61, 115.99, 130.87, 131.03, 134.09, 135.87, 136.15, 146.70, 149.05, 151.96, 151.97, 154.61, 159.07, 166.96, 168.32, 170.47, 170.53; MS (pos. FAB): *m/z* (%): 733 (100, $[M+H]^+$), 507 (13); HR-MS (pos. FAB) $C_{35}H_{44}N_{10}O_8$: calcd for $[M+H]^+$: 733.3422; found: 733.3426.

Model compound 24: Compound **24** was prepared similar to compound **2**. As the dimer carboxylic acid the *trans-syn*-compound **17** (55 mg, 0.15 mmol) was used. The crude product **24** was dissolved in a small amount of methanol and precipitated through addition of diethyl ether. Compound **24** was obtained after column chromatography on silica gel (silica gel-H, d = 3 cm, L = 20 cm, $CHCl_3$/MeOH 7:1) as a yellow powder (35 mg, 32 %). R_f ($CHCl_3$/MeOH 10:1) = 0.28; m.p.: 200 – 202 °C; IR (KBr): 3430*m*, 3200*m*, 3078*w*, 2956*w*, 2922*w*, 2856*w*, 1700*s*, 1650*s*, 1578*m*, 1548*s*, 1473*m*, 1406*w*, 1372*w*, 1355*m*, 1289*m*, 1224*m*, 1150*w*, 1094*w*, 933*w*; ^{1}H NMR (500 MHz, [D$_6$]DMSO): δ = 0.86 (t, J = 7.1 Hz, 3H), 1.16 (t, J = 7.1 Hz, 3H), 1.20 (s, 3H), 1.23 (m, 4H), 1.27 (s, 3H), 1.38 (m, 2H), 2.41 (s, 3H), 2.51 (s, 3H), 3.02 (m, 2H), 3.48 (q, J = 6.9 Hz, 2H), 3.65 (d, J = 8.2 Hz, 1H), 3.73 (d, J = 16.6 Hz, 1H), 3.85 (d, J = 16.6 Hz, 1H), 3.87 (d, J = 8.2 Hz, 1H), 3.93 (q, J = 7.1 Hz, 2H), 3.97 (d, J = 16.5 Hz, 1H), 4.00 (d, J = 16.5 Hz, 1H), 4.63 (t, J = 6.9 Hz, 2H), 7.87 (t, J = 5.8 Hz, 1H), 7.92 (s, 1H), 7.93 (s, 1H), 8.25 (t, J = 6.0 Hz, 1H), 10.46 (s, 1H), 10.50 (s, 1H); ^{13}C NMR (125 MHz, [D$_6$]DMSO): δ = 12.82, 13.80, 18.71, 20.70, 20.83, 21.16, 21.73, 28.47, 28.59, 35.45, 35.83, 38.52, 42.93, 45.38, 45.40, 45.59, 49.13, 63.77, 63.87, 115.98, 130.86, 131.03, 134.03, 135.93, 136.05, 146.69, 148.76, 151.22, 151.44, 154.52, 159.07, 167.63, 168.98, 170.73, 170.79; MS (pos. FAB): *m/z* (%): 733 (26, $[M+H]^+$), 507 (100), 480 (10), 338 (9); HR-MS (pos. FAB) $C_{35}H_{44}N_{10}O_8$: calcd for $[M+H]^+$: 733.3422; found: 733.3423.

Oligonucleotide synthesis: Oligonucleotide synthesis was performed on a Pharmacia-Gene-Plus synthesizer connected to a Olivetti-M 300 personal computer. Synthesis of the oligonucleotides **25** – **32** was performed by using a modified 1.3 μmol cycle and Pac-amidites. Solvents and solutions were made according to the manufacturers protocol. The phosphoramidite (0.1 M in MeCN) and 1*H*-tetrazole (0.5 M in MeCN) solution were equal in concentrations to those used for the synthesis of natural oligodeoxynucleotides. Average coupling yields monitored by on-line trityl assay were generally in the range of 95 – 99 %. All syntheses were run in the trityl-on mode, resulting **DMTr-25** – **DMTr-32**. For the deprotection and cleavage of **DMTr-26** and **DMTR-28** from the support, the solid support was suspended in sat. NH_3/MeOH (1 mL, MeOH dried over 3 Å molecular sieves) and kept at 25 °C with occasional shaking for one day. For the deprotection and purification of all other oligonucleotides, the solid support was suspended in conc. aqueous NH_3/MeOH = 3:1 (2 mL) and left for 5 h at 55 °C to effect deprotection and cleavage. After addition of 1 M NEt_3/HOAc (2 mL) to each solution, the support was filtered off and washed with water (3 × 0.5 mL). The solution was concentrated to 1 mL and the oligonucleotides were purified by HPLC (C_{18}-RP, A: 0.1 M NEt_3/HOAc, B: 80 % MeCN, 25 →40 % B in 40 min). After removal of the solvent in vacuo, all oligonucleotides were detritylated by addition of 50 % HCOOH/H_2O (3 mL). After 5 min the formic acid was removed in vacuo and **25** – **32** were purified by HPLC (C_{18}-RP, 5 →10 % B in 5 min, 10 →25 % B in 30 min). Laser-desorption mass spectra (negative ions detected): calcd for **25**: 3595.5, found: 3596.1; calcd for **26**: 3567.4, found: 3567.9; calcd for **27**: 4168.8, found: 4168.3; calcd for **28**: 4140.8, found: 4140.0; calcd for **29**: 3595.5, found: 3596.4; calcd for **31**: 4168.8, found: 4170.5.

Enzymatic studies: 500 μL solutions containing the damaged oligonucleotide (1 – 5 μmol), 0.1 M NaCl, 10 mM KH_2PO_4 pH 7.0, and 5 mM DTT and DNA-photolyase (25 nM or 50 nM) were prepared and filled into a quartz cuvette equipped with a magnetic stirrer. The enzyme was added in the dark. The assay solutions were mixed and irradiated at 435 nm (*A. nidulans*). For each time point 20 μL were removed and 0.1 M HOAc (10 μL) was added in order to keep the enzyme reaction stopped. The samples were analyzed by reversed-phase HPLC or ion-exchange chromatography. Reversed phase: Nucleosil 120-3, C18 (250 × 4 mm), 0.7 mL min^{-1}, A: 20 mM NH_4OAc, B: 50 % MeCN, 50 % A (*v*/*v*), 0 →20 min: 6 →16 % B. Retention times: **25**: 7.7 min, **26**: 6.8 min, **27**: 13.3 min, **28**: 12.2 min, **29**: 10.8 min, **30**: 9.8 min, **31**: 17.6 min, **32**: 14.6 min. Ion-exchange chromatography: Nucleogel SAX 1000-8/77, 2 mL min^{-1}, A: 0.2 M NaCl, 10 mM Na_2HPO_4, pH 11.4, B: 1 M NaCl, 10 mM Na_2HPO_4, pH 11.4, 0 →6 min: 100 % A, 6 →23 min: 0 →51 % B. Retention times: **25**: 14.8 min, **26**: 15.0 min, **27**: 18.0 min, **28**: 18.0 min, **29**: 17.1 min, **30**: 17.2 min, **31**: 19.6 min, **32**: 19.5 min

Acknowledgment

This work was supported by the Schweizer Nationalfond, by the ETH Zürich and the Boehringer Ingelheim Fonds (Doctoral Scholarship to J.B.). We thank Prof. F. Diederich for the continuing generous support and Prof. U. Wild for enabling us to perform the GAMESS(US) calculations (E.-U.W.). We thank M. Leduc for a careful inspection of the manuscript.

[1] P. F. Heelis, R. F. Hartman, S. D. Rose, *Chem. Soc. Rev.* **1995**, 289 – 297.
[2] S.-T. Kim, A. Sancar, *Photochem. Photobiol.* **1993**, *57*, 895 – 904.
[3] T. Carell, *Angew. Chem.* **1995**, *107*, 2697 – 2700; *Angew. Chem. Int. Ed. Engl.* **1995**, *34*, 2491 – 2494.
[4] J.-S. Taylor, *Acc. Chem. Res.* **1994**, *27*, 76 – 82.
[5] J.-S. Taylor, *J. Chem. Educ.* **1990**, *67*, 835 – 841.
[6] T. Carell, *Chimia* **1995**, *49*, 365 – 373.
[7] A. Sancar, *Biochemistry* **1994**, *33*, 2 – 9.
[8] E. C. Friedberg, G. C. Walker, W. Siede, *DNA repair and mutagenesis*, ASM Press, Washington, D.C. **1995**.
[9] M. Prather, P. Midgley, F. S. Rowland, R. Stolarski, *Nature* **1996**, *381*, 551 – 554.
[10] H. Slaper, G. J. M. Velders, J. S. Daniel, F. R. deGruijl, J. C. van der - Leun, *Nature* **1996**, *384*, 256 – 258.
[11] R. Epple, E.-U. Wallenborn, T. Carell, *J. Am. Chem. Soc.* **1997**, *119*, 7440 – 7451.
[12] I. D. Podmore, P. F. Heelis, M. C. R. Symons, A. Pezeshk, *Chem. Commun.* **1994**, 1005 – 1006.
[13] S.-T. Kim, A. Sancar, *Biochemistry* **1991**, *30*, 8623 – 8630.
[14] D. L. Svoboda, C. A. Smith, J.-S. Taylor, A. Sancar, *J. Biol. Chem.* **1993**, *268*, 10684 – 10700.
[15] A. A. Voityuk, N. Rösch, *J. Phys. Chem. A* **1997**, *101*, 8335 – 8338.
[16] A. A. Voityuk, M. E. Michel-Beyerle, N. Rösch, *J. Am. Chem. Soc.* **1996**, *118*, 9750 – 9758.
[17] J. Hahn, M.-E. Michel-Beyerle, N. Rösch, *J. Phys. Chem. B* **1999**, *103*, 2001 – 2007.
[18] T. Langenbacher, X. Zhao, G. Bieser, P. F. Heelis, A. Sancar, M. E. Michel-Beyerle, *J. Am. Chem. Soc.* **1997**, *119*, 10532 – 10536. This study was performed with the *E. coli* enyzme and dinucleotide cyclobutane substrates. For calculations see: D. B. Sander, O. Wrest, *J. Am. Chem. Soc.* **1999**, *121*, 5127 – 5134.
[19] A. P. M. Eker, P. Kooiman, J. K. C. Hessels, A. Yasui, *J. Biol. Chem.* **1990**, *265*, 8009 – 8015.
[20] J. Butenandt, L. T. Burgdorf, T. Carell, *Angew. Chem.* **1999**, *111*, 718 – 721; *Angew. Chem. Int. Ed.* **1999**, *38*, 708 – 711.
[21] J. Butenandt, A. P. M. Eker, T. Carell, *Chem. Eur. J.* **1998**, *4*, 642 – 653. The thymidine dimer was prepared as described for the uridine dimer. All details and the analytical data will be reported in due course.
[22] T. Carell, R. Epple, V. Gramlich, *Helv. Chim. Acta* **1997**, *80*, 2191 – 2203.
[23] A. G. Cochran, R. Sugasawara, P. G. Schultz, *J. Am. Chem. Soc.* **1988**, *117*, 5453 – 5461.
[24] J. R. Jacobsen, A. G. Cochran, J. C. Stephans, D. S. King, P. G. Schultz, *J. Am. Chem. Soc.* **1995**, *118*, 5453 – 5461.

  0947-6539/00/0601-0071 $ 17.50+.50/0

[25] R. Kuhn, W. v. Klaveren, *Ber. Dtsch. Chem. Ges.* **1938**, *71*, 779 – 780.
[26] T. Carell, J. Butenandt, *Angew. Chem.* **1997**, *109*, 1590 – 1593; *Angew. Chem. Int. Ed. Engl.* **1997**, *36* 1461 – 1464.
[27] T. Carell, H. Schmid, M. Reinhard, *J. Org. Chem.* **1998**, *63*, 8741 – 8747.
[28] C. Petry, Dissertation, Ruprecht-Karls-Universität Heidelberg, **1993**, p. 186.
[29] R. Kuhn, F. Weygand, *Ber. Dtsch. Chem. Ges.* **1934**, *67*, 1409 – 1413.
[30] R. Kuhn, F. Weygand, *Ber. Dtsch. Chem. Ges.* **1935**, *68*, 1282 – 1288.
[31] B. Castro, G. Evin, C. Delve, R. Seyer, *Synthesis* **1977**, 413 – 469.
[32] C. G. Hatchard, C. A. Parker, *Proc. R. Soc. A.* **1956**, *235*, 518 – 536.
[33] H. G. O. Becker, *Einführung in die Photochemie*, Deutscher Verlag der Wissenschaften, Berlin, **1991**.
[34] C. Reichardt, *Solvents and Solvent Effects in Organic Chemistry*, VCH, Weinheim, **1988**.
[35] R. F. Hartman, S. D. Rose, *J. Am. Chem. Soc.* **1992**, *114*, 3559 – 3560.
[36] I. Husain, A. Sancar, *Nucleic Acids Res.* **1987**, *15*, 1109 – 1120.
[37] H.-W. Park, S.-T. Kim, A. Sancar, J. Deisenhofer, *Science* **1995**, *268*, 1866 – 1872.
[38] T. Tamada, K. Kitadokoro, Y. Higuchi, K. Inaka, A. Yasui, P. E. de Ruiter, A. P. M. Eker, K. Miki, *Nature Struct. Biol.* **1997**, *11*, 887 – 891.
[39] R. F. Hartman, J. R. van Camp, S. D. Rose, *J. Org. Chem.* **1987**, *52*, 2684 – 2689.
[40] S.-T. Kim, S. D. Rose, *J. Phys. Org. Chem.* **1990**, *3*, 581 – 586.
[41] I. Mayer, *Int. J. Quant. Chem.* **1986**, *29*, 477 – 483.
[42] F. E. Hruska, L. Voituriez, A. Grand, J. Cadet, *Biopolymers* **1986**, *25*, 1399 – 1417.
[43] K. McAteer, Y. Jing, J. Kao, J.-S. Taylor, M. A. Kennedy, *J. Mol. Biol.* **1998**, *282*, 1013 – 1032.
[44] B. J. V. Berg, G. B. Sancar, *J. Biol. Chem.* **1998**, *273*, 20276 – 20284.
[45] R. J. Roberts, *Cell* **1995**, *82*, 9 – 12.
[46] G. L. Verdine, S. D. Bruner, *Chem. Biol.* **1997**, *4*, 329 – 334.
[47] A. S. Jones, P. Lewis, S. F. Withers, *Tetrahedron* **1973**, *29*, 2293.
[48] M. W. Schmidt, K. K. Baldridge, J. A. Boatz, S. T. Elbert, M. S. Gordon, J. H. Jensen, S. Koseki, N. Matsunaga, K. A. Nguyen, S. J. Su, T. L. Windus, M. Dupuis, J. A. Montgomery, *J. Comput. Chem.* **1994**, *14*, 1347 – 1363.

Received: April 26, 1999 [F 1745]

0947-6539/00/0601-0072 $ 17.50+.50/0